RESEARCH PAPER

Synthesis of $ZrSe_2$ Nanoparticles by Hydrothermal Method for Gas Sensing Applications

Tushar Satish Wagh[1], Sagar Hiraman Mane[2], Gotan Hiralal Jain[3], Madhavrao Keshavrao Deore[4,*]

* *deoremadhav63@gmail.com*

[1] Department of Physics, Deola Education Society's Karmaveer Ramraoji Aher ASC College, Deola, Tal. -Deola, Dist.-Nashik, Maharashtra-423102, India

[2] Department of Physics, MVP's K.A.A.N.M. Sonawane ACS College, Satana, Tal. -Satana, Dist.-Nashik, Maharashtra-423301, India

[3] Department of Physics, Maratha Vidya Prasarak Samaj's Arts, Commerce and Science College, Nandgaon, Tal. - Nandgaon, Dist.- Nashik, Maharashtra-423106, India

[4] Material Research Laboratory, MVP's, K.R.T. Arts, B.H. Commerce, A.M. Science College, Nashik, Shivajinagar, Gangapur Road, Nashik-422002, India

Received: April 2024 **Revised: September 2024** **Accepted: September 2024**

DOI: 10.22068/ijmse.3601

Abstract: *Nowadays metal oxide nanoparticles and transition metal dichalcogenides play a vital role in various areas like optical sensors, solar cells, energy storage devices, gas sensors and biomedical applications. In the current research work, we synthesized $ZrSe_2$ nanoparticles by hydrothermal method. The $ZrSe_2$ nanoparticles were synthesis using precursors such as $ZrOCl_2.8H_2O$ and $Na_2SeO_3.5H_2O$ in the addition of surfactant cetyl trimethyl ammonia bromide CTAB and reductant hydrazine hydrate, respectively. Synthesized $ZrSe_2$ nanopowder thick films were developed on a glass substrate using the screen printing method. The structural properties of $ZrSe_2$ powder were studied by X-ray diffraction (XRD). The X-ray diffraction analysis revealed that the hexagonal crystal structure and crystalline size were found to be 55.75 nm. The thick films of $ZrSe_2$ were characterized by field emission scanning electron microscopy (FESEM) and energy dispersive X-ray analysis (EDAX). The surface morphological analysis of $ZrSe_2$ nanostructured thick film shows hierarchical nanoparticles. The energy band gap of synthesized powder was calculated using a Tauc plot from UV-visible spectroscopy. The gas-sensing properties of $ZrSe_2$ thick films were studied. The developed $ZrSe_2$ thick films show maximum sensitivity and selectivity towards the ammonia NH_3 gas at an operating temperature of 120°C and the gas concentration was 500 ppm. The developed thick films show fast response and recovery time.*

Keywords: *Hydrothermal method, Transition metal dichalcogenides, Thick films, Gassensor, Tauc, plot, Sensitivity.*

Graphical abstract:

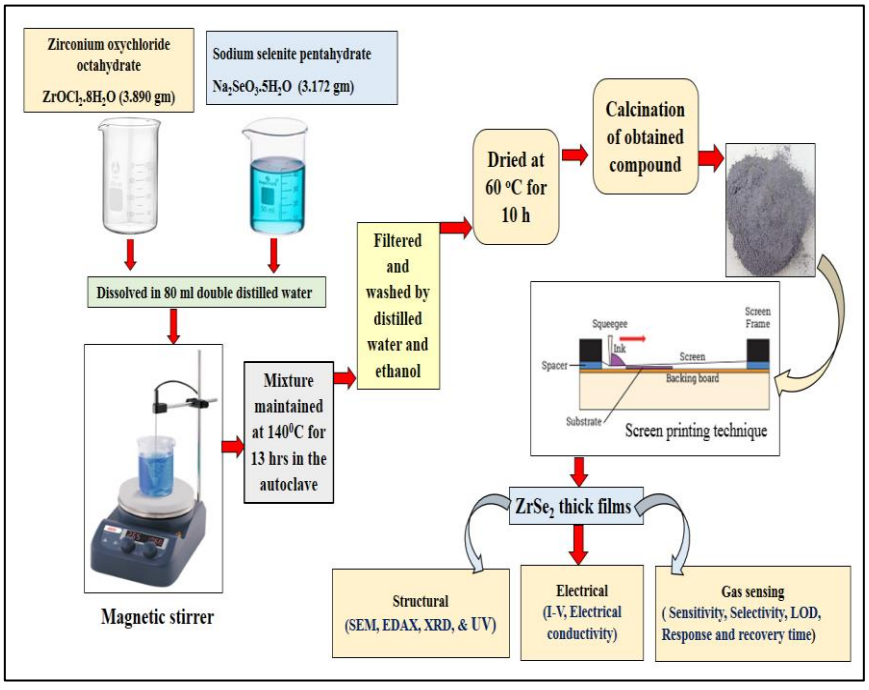

[DOI: 10.22068/ijmse.3601]

1. INTRODUCTION

For the last two or three decades environmental pollution has been a series problem when we relate it to human health issues. Air pollution has been a critical issue in the metro cities where industrial gases and automobile gases are released into the air and these gases are harmful to the human health. Therefore most of the researchers focused on to work on the detection of hazardous gases by synthesis of novel materials. Nowadays in material research, scientists focus on designing the material to detect hazardous gases by fabricating the gas sensor [1].

Transition metal dichalcogenides (TMDCs) may be a kind of promising substance due to their high surface-to-volume ratio and interesting band structures with tunable band gaps material that are more beneficial to designing gas sensors. TMDCs can be used for toxic gas detection and adsorption because of their high sensitivity to the environment [1, 2]. They are a class of layered materials made up of a transition metal sandwiched between atoms of chalcogen by chemical bonding, producing X-M-X layers that are kept together by weak van der Waals forces [2]. TMDCs exhibit variable band gaps from 0 to 3 eV, which can be tuned by defects, thickness, lattice point variations and morphology. Layer-dependent properties in conjunction with surface structure modification, and chemical doping were investigated to improve the sensing performance of the TMDCs [3].

Zirconium selenide ($ZrSe_2$) is a group IV TMDC the famous semiconducting materials, metallic and superconducting properties and its physical properties have been constantly investigated during recent years. The $ZrSe_2$ crystallises in a hexagonal CdI_2 layer structure [4]. $ZrSe_2$ is a class of TMDCs with a moderate bandgap, semiconducting nature and good electrical characteristics. Zirconium diselenide ($ZrSe_2$) has attracted due to its unique optical, structural and electronic properties. The structure is composed of sheets of Zr atoms coordinated octahedrally by Se atoms, where each Se atom is bonded to three Zr atoms via van der Waals interaction. $ZrSe_2$ is an n-type semiconductor material donating an electron to it increases the conductivity [5].

In the current work, we reported a novel synthesis method for the synthesis of the $ZrSe_2$ nanoparticles using a hydrothermal method and then fabricated them using screen printing techniques onto a glass substrate. The $ZrSe_2$ nanopowder materials were examined using X-ray diffraction (XRD) and UV-visible spectroscopy (UV) for their structural and optical properties. The surface morphology properties of the $ZrSe_2$ thick film were studied using scanning electron microscopy (FESEM). This study discusses the $ZrSe_2$ thick film-based gas-sensing properties, including sensitivity, selectivity, gas concentration, stability, response, and recovery time. The sensing response for different concentrations of NH_3 gas was investigated for the $ZrSe_2$ thick film sensor. Also, the gas-sensing properties of $ZrSe_2$ thick films for various gases such as NH_3, NO_2, LPG and C_2H_6O were tested.

2. EXPERIMENTAL PROCEDURES

2.1. Synthesis of $ZrSe_2$ Nanoparticles Using Hydrothermal Method

All the chemicals used in the experiments were of analytical grade and used without further purification. In a typical synthesis, 3.890 g of $ZrOCl_2.8H_2O$, and 3.172 g $Na_2SeO_3.5H_2O$ were dissolved in 80 ml of double distilled water under constant magnetic stirring at room temperature for 45 min. Then an appropriate quantity of CTAB was added to the above solution. After stirring the solution for 15 min, 1 ml hydrazine was added drop-wise into the mixture and the colour of the solution became peach precipitate, then the pH of the solution was 9. The resulting solution was transferred to a 200 ml Teflon-lined stainless-steel autoclave, sealed tightly and maintained at 140°C for 13 hrs, then cooled down to room temperature naturally. The resulting black precipitates were filtered, washed with double distilled water and absolute ethanol and then dried for 10 hrs at 60°C. After that, the obtained precipitate or compound was calcined at 200°C for 3 Hrs and then ground using mortar and pestle for 2 Hrs [6, 7]. Finally, $ZrSe_2$ nanopowder was obtained. The $ZrSe_2$ nanopowder was further used to develop thick films using the screen printing technique.

2.2. Thick Film Preparation

The thick films of synthesized $ZrSe_2$ nanopowder were developed on a glass substrate using a screen printing technique. All films were

[DOI: 10.22068/ijmse.3601]

developed on a glass substrate. The 30% and 70% ratios of organic and inorganic materials were used for the preparation of thick films. In organic material, ethyl cellulose and butyl carbitol acetate were used to make thixotropic paste. After that thick films were developed/prepared using a screen printing setup. After successfully preparing of films, prepared films were dried under an IR lamp to remove contaminations. Then finally films were annealed at 200°C for 2 hours using a muffle furnace [8, 9].

2.3. Characterization of Synthesized $ZrSe_2$ Powder

To confirm the nanostructure of synthesised particles or powder standard characterizations have been adopted. In standard characterizations, XRD, FESEM, EDX and UV spectroscopy such types of techniques were used. The X-ray powder diffractometer (XRD), Bruker Analytical Instruments Pvt. Ltd., Germany, Model: D8 Advance) with Cu-Kα radiations having λ= 1.5418 was used to record the XRD pattern of the $ZrSe_2$ powder in the 2θ range 10-80° in a step size range of 0.020°/s. A FESEM (JEOL/EO, JSM-6390) was used to capture the surface morphological micrograph of the thick film with an operating acceleration voltage of 20 KV. Elemental analysis was done through energy-dispersive by X-ray (OXFORD instrument). The UV-visible spectrum analysis was performed to determine the band gap of the synthesized $ZrSe_2$ nanoparticles. Furthermore, the electrical characterization and electrical conductivity carried out of thick films of $ZrSe_2$ by using the static electrical and gas sensing system [9]. The schematic of the static electrical and gas sensing system experimental setup is shown in Fig. 1.

The static gas and electric system consists of a tightly closed glass chamber and two sample holders. The film was placed in a glass chamber using sample holders. The heater coil is situated in the glass chamber which is connected to the dimmer stat (230 VAC power supply) for controlling the coil voltage. According to the provided power supply to the coil, the coil is heated and produces heat (temperature) inside the glass chamber. The temperature inside the glass chamber or film surrounding temperature was measured by a digital temperature indicator. In a digital temperature indicator, a Chromium-Aluminum thermocouple is used to sense surrounding temperature. The influence of temperature on the conductance of the films is measured using pico-ammeter [9, 10].

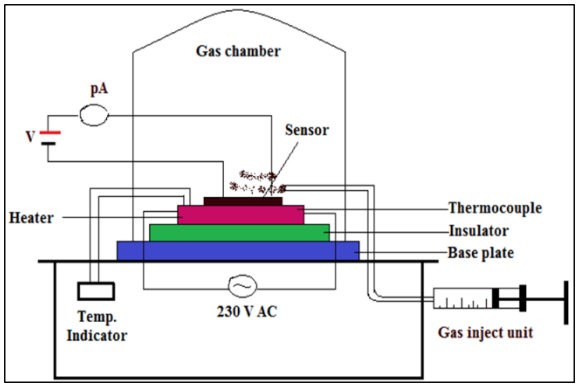

Fig. 1. Schematic of static electrical and gas sensing system.

The BET (Brunauer-Emmett-Teller) method for analyzing specific surface area is conducted using a specialized instrument designed to measure the gas adsorption characteristics of a material. This instrument typically features a gas adsorption chamber where the sample is exposed to a specific gas, often nitrogen or argon, at controlled temperatures. The chamber is equipped with a vacuum system to degas the sample before the analysis, ensuring that any pre-existing adsorbates are removed. The gas manifold system precisely controls the flow of gas and adjusts the pressure to measure the adsorption isotherms.

The data acquisition and analysis software processes these measurements to calculate the specific surface area based on the BET equation. Additionally, the instrument includes a temperature control system to maintain consistent conditions throughout the analysis, ensuring accurate and reliable results. The schematic of the BET method apparatus with its working is illustrated in Fig. 2.

3. RESULTA AND DISCUSSION

3.1. Structural Characterizations

3.1.1. X-ray diffractometer

The XRD pattern of the $ZrSe_2$ powder is shown in Fig. 3 and the results indicate that the $ZrSe_2$ material has a crystalline structure and grows with a hexagonal structure.

[DOI: 10.22068/ijmse.3601]

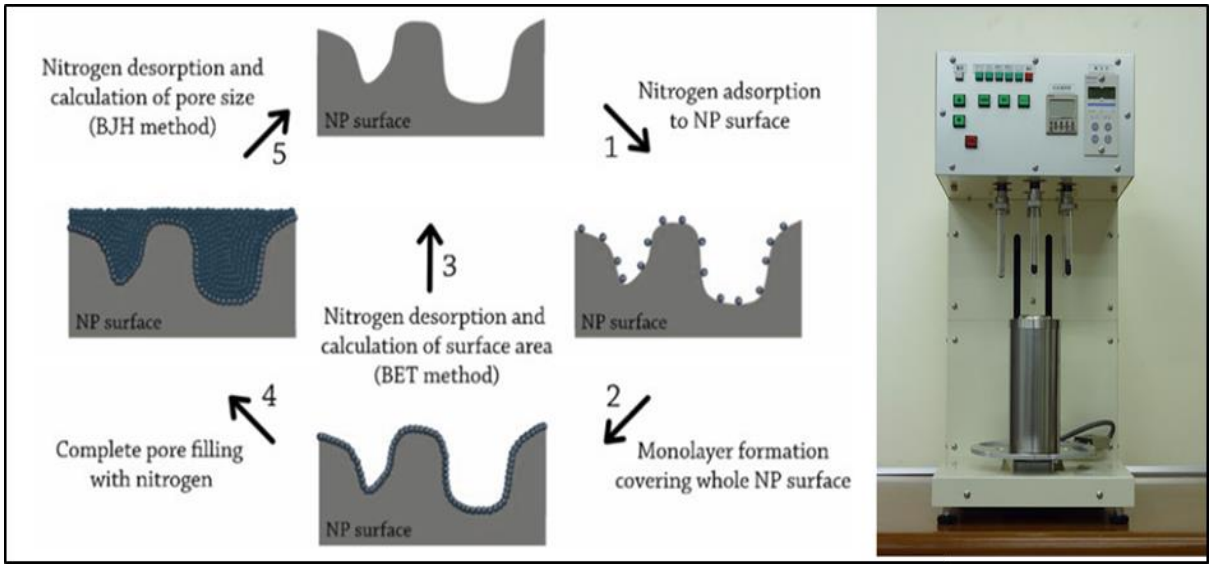

Fig. 2. Schematic of BET method apparatus

The significant peaks for $ZrSe_2$ were found to be at (002), (011), (012), (003), (111), (103), (112) and (004) which corresponds to 2θ angles of 28.25°, 30.15°, 39.77°, 43.70°, 50.30°, 51.95°, 56.83° and 59.67° respectively.

The obtained peaks of $ZrSe_2$ match with the JCPDS Card No. 03-065-3376 [11]. The higher peak intensities in the XRD pattern indicate a greater crystallinity of the material. The preferred orientation is along the (011) plane.

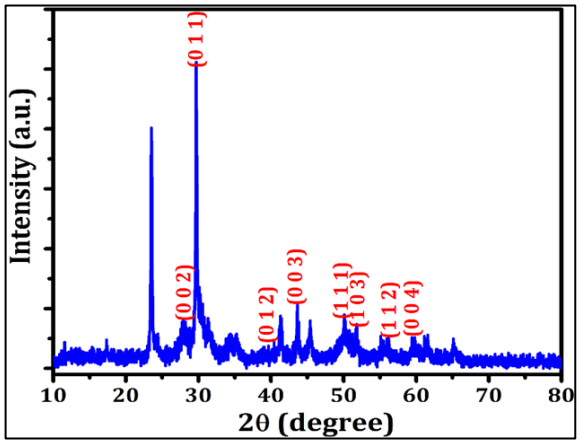

Fig. 3. XRD pattern of $ZrSe_2$ thick films.

The presence of prominent peaks is important as it produces a large surface area for an effective gas-sensing mechanism. From X-ray diffraction data, the crystallite size was calculated using Debye–Scherrer formula in Eq. 1.

$$D = 0.9\,\lambda/\beta\,\mathrm{Cos}\,\theta \quad (1)$$

Where λ is the wavelength of the CuKα target used, β is the full width at half maximum of the peak in radians and θ is Bragg's diffraction angle at peak position in degrees [8]. From XRD the crystallite size was found to be 55.75 nm.

3.1.2. UV-visible spectroscopy

The absorption versus wavelength spectrum of the $ZrSe_2$ thick films is shown in Fig. 4. The range of wavelength is varied from 250 nm to 900 nm.

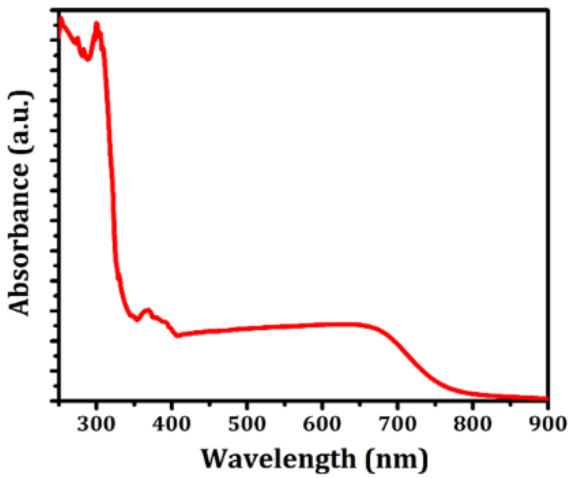

Fig. 4. UV-visible absorbance spectra.

The absorption data was analyzed by using a classical relation Eq. 2.

$$\alpha = A(h\nu - Eg)^n/h\nu \quad (2)$$

Where n= 2 & α= absorption coefficient in the order of 10^4 cm^{-1} for direct allowing transition. The band gap of the $ZrSe_2$ thick film was plotted

[DOI: 10.22068/ijmse.3601]

by drawing an intercept of the plot between ($\alpha h\upsilon^2$) on the y-axis and ($h\upsilon$) on the x-axis as shown in Fig. 5. By using the Tauc plot method optical band gap was calculated. The nature of the plots suggests a direct interband transition. The optical band gap of $ZrSe_2$ thick film was found to be 3.75 eV [11].

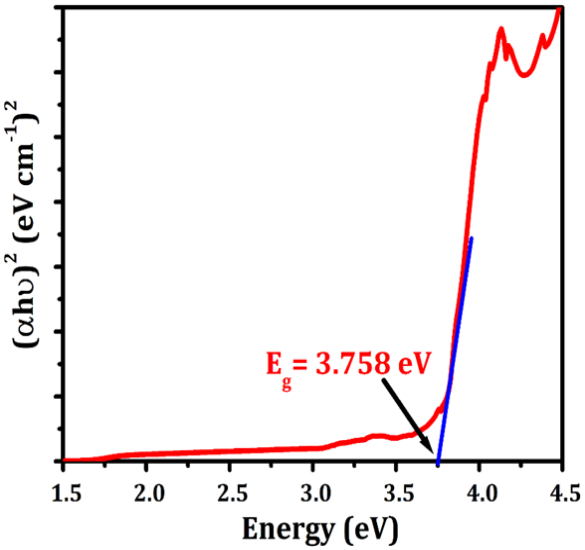

Fig. 5. Plot of $(\alpha h\upsilon)^2$ versus ($h\upsilon$) for $ZrSe_2$ thick film.

3.1.3. Field emission scanning electron microscopy

Fig. 6 (a-b) represents the SEM micrograph of the $ZrSe_2$ thick films. The results show that its hierarchical nanoparticles formed viz. nanorods, and nanoflakes [11, 12]. In the morphology of nanoparticles homogenous and well-distributed surface was detected. The influence of precursor is found in the SEM micrographs. The average particle diameter size observed in SEM images was 750 nm. The specific surface area is calculated by the BET method [8, 9] and it was found to be 26.86 m^2/gm. The specific surface area plays an important role in the gas-sensing mechanism because if the specific surface area of a nanoparticle increases the adsorption rate of oxygen vacancies increases on the surface of particles during gas sensing reaction or process [9].

3.1.4. Energy dispersive X-ray analysis

Energy dispersive X-ray (EDX) analysis was performed in addition to FESEM analysis to evaluate the elemental composition of $ZrSe_2$ thick films under an acceleration voltage of 20 keV, as shown in Fig. 7. The atomic weight percentage for these elements shows a nonstoichiometric nature as shown in Table 1.

Table 1. Elemental analysis from EDX

Element	At. %	Wt.%
Se	34.42	31.24
Zr	65.58	68.76

3.2. Electrical Properties

In gas sensors electrical parameters of the prepared films play a key role in gas sensing mechanisms. The transition metal dichalcogenides have differentiated in 2D nanoparticles based on their conductivity, chemical compositions and structural alignments, based on these properties of TMDCs, they are classified into as metallic, semi-metallic, semiconducting, insulating, or superconducting [12].

The electrical transfer characteristics of TMDCs are useful in many applications like nanodevices, thin film transistors and others. The electrical properties of fabricated $ZrSe_2$ thick films were studied using a static gas system.

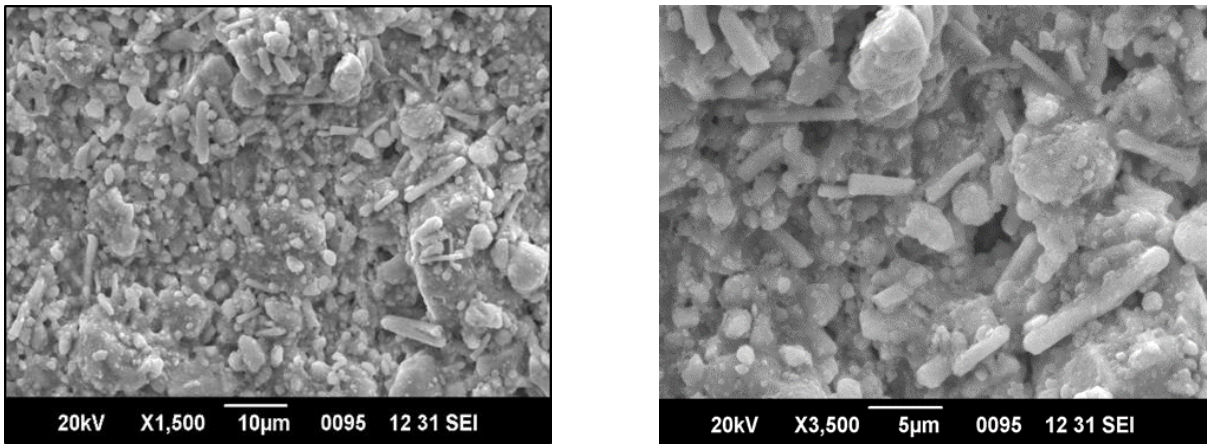

Fig. 6. (a-b) SEM micrograph of $ZrSe_2$ thick film.

[DOI: 10.22068/ijmse.3601]

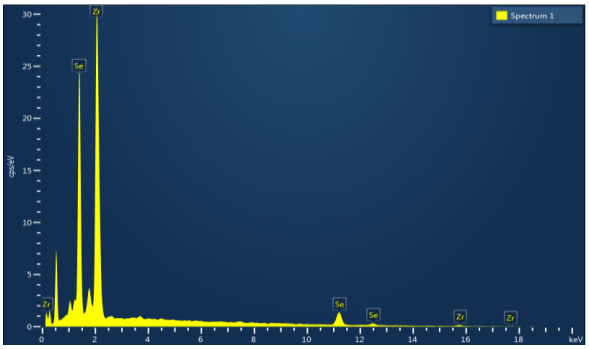

Fig. 7. EDX pattern of $ZrSe_2$ thick films.

3.2.1. I-V characteristics of the $ZrSe_2$ thick films

The I-V characteristic of the $ZrSe_2$ thick film is illustrated in Fig. 8. It is found that the electric current is directly proportional to the applied potential. I-V characteristics of the $ZrSe_2$ thick film show an ohmic behaviour for both –ve and +ve applied potential [13]. The thick film resistance is found to be high, hence the current through the $ZrSe_2$ thick film is found in the pico ampere range. As an applied voltage is changed the amount of current in pico ampere also changes.

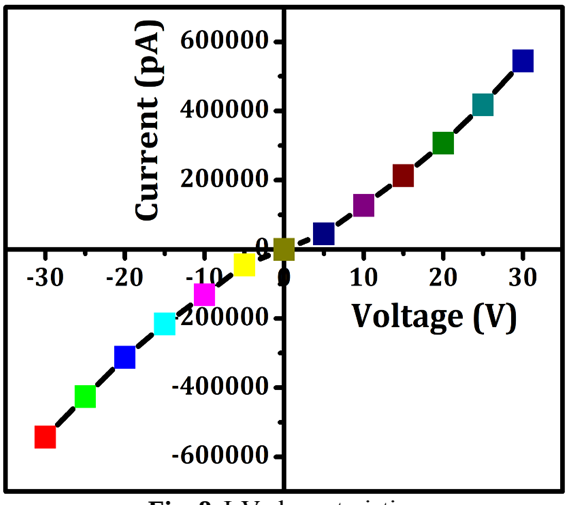

Fig. 8. I-V characteristics

3.2.2. Electrical conductivity

The conductivity of the films is inversely proportional to the resistivity. The resistivity of the film depends on the mobility of charge carriers present in the material. The resistance of the film depends upon the surrounding temperature. The variation of electrical conductivity with the temperature of $ZrSe_2$ thick film at constant potential. The conductivity of the thick film was calculated using Eq. 3.

$$\sigma = l/(R\ b\ t) \quad (3)$$

The electrical conductivity of $ZrSe_2$ thick films was determined by increasing the surrounding temperature of the film. Fig. 9 reveals the plot of the Log of conductivity Vs 1000/T°K of $ZrSe_2$ thick films.

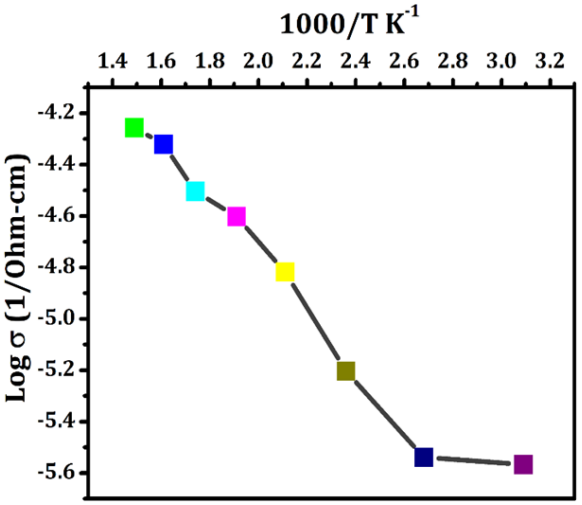

Fig. 9. Variation of Log of conductivity Vs 1000/T°K^{-1} of $ZrSe_2$ thick film

It is observed that, as the surrounding temperature raised the conductivity of the $ZrSe_2$ thick films also raised. This electrical nature of $ZrSe_2$ thick films attributed semiconducting behaviours of prepared films and films shows a negative temperature coefficient of resistance. As ambient temperature increases then film resistance goes on decreases this phenomenon is attributed to the NTC of films [13, 14]. The observed increase in conductivity with temperature may be caused by the entrapped electrons being thermally agitated as the temperature rises and the rate of oxygen ions being adsorbed increasing, which releases the flow of electrons into the conduction band and enhances current [10, 15].

3.3. Gas-Sensing Properties

The gas sensing performance of $ZrSe_2$ thick films was studied by using a static gas sensing system as shown in Fig. 1. The gas sensing system consists of the glass dome, gas supply valves, heating system, temperature controller, power supply and digital pico ammeter. A heater is fixed at the base plate with the applied AC voltage to heat the gas sensor at the required operating temperatures. The output of the thermocouple

[DOI: 10.22068/ijmse.3601]

was used to indicate the temperature by the temperature indicator. A gas inlet valve is also fitted at the base plates and injecting the gas at the required operating temperature.

The prepared $ZrSe_2$ thick films were tested for ammonia (NH_3), nitrogen dioxide (NO_2), liquefied petroleum gas (LPG), and ethanol (C_2H_6O) gases. The films were tested at different gas concentrations and different operating temperatures. The gas sensing study was carried out to determine the sensitivity, selectivity, limit of detection, reusability, response and recovery time of the prepared $ZrSe_2$ thick films.

3.3.1. *Sensitivity*

The sensitivity of the film to a target gas is defined as the ratio of the change in conductance of a film upon exposure of the gas to the original conductance in air, which can be calculated by Eq. 4.

$$\text{Sensitivity}\ (\%) = (|Ig - Ia|/Ia)\ X\ 100 \qquad (4)$$

Where, Ig- current/conductance in the presence of target gas and Ia- current in air.

Fig. 10 shows the sensitivity versus operating temperature graph of $ZrSe_2$ thick films. The $ZrSe_2$ thick films show maximum sensitivity to NH_3 gas as compared to other selected gases. The Maximum Sensitivity was found to be 78.19% to ammonia gas at an operating temperature of 120°C and the gas concentration of NH_3 was 500 ppm. It is also observed from Fig. 10, that initially, $ZrSe_2$ thick films showed poor sensitivity to NH_3 gas up to 80°C then at 120°C more sensitivity was recorded and after 80°C again the sensitivity of the film declined. It could be 120°C operating temperature is suitable for the adsorption rate of NH_3 gas molecules. At 120°C the maximum charge carriers are activated and produce a fast response to the gas [14, 16]. Because of the function of temperature adsorption-desorption behaviour of gas on sensing materials, the sensing properties are significantly reliant on operating temperature. Hence, to further investigate the properties of the $ZrSe_2$ thick film, the optimal operating temperature of 120°C gives maximum sensitivity. This is because there are a lot of charge carriers (e^-), which causes the sensor resistance to fluctuate quickly. It is well recognized that oxygen adsorption and desorption on the surface of the sensing materials play a major role in the variation in resistance for film. The adsorbed oxygen may desorb above the optimal operating temperature or the oxygen species may predominate at the film surface, which could elucidate the diminishing gas sensitivity at higher temperatures [15, 16].

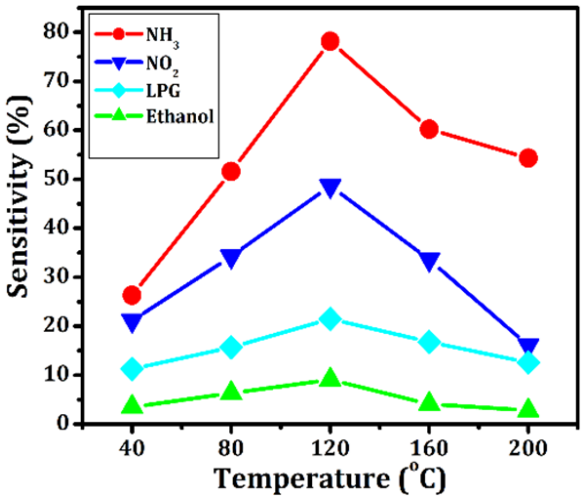

Fig. 10. Sensitivity versus operating temperature plot of $ZrSe_2$ thick films.

3.3.2. *Selectivity*

Selectivity is the property of a sensor or thick film that allows it to detect one gas while suppressing other targeted gases. Fig. 11 shows the selectivity histogram of $ZrSe_2$ thick films to selected gases.

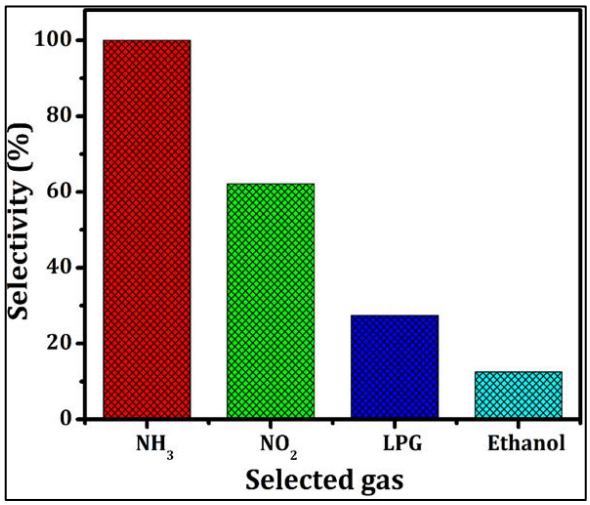

Fig. 11. Selectivity plot

The selectivity of the film strongly depends on the sensitivity of the film. The maximum selectivity was found to be NH_3 gas hence 100% has been considered to be NH_3 gas. Ethanol gas shows poor selectivity because it has very little sensitivity to targeted gases. It is observed from Fig. 11, that the $ZrSe_2$ thick films give maximum response to NH_3

[DOI: 10.22068/ijmse.3601]

gas at an operating temperature of 120°C and the gas concentration of NH_3 was 500 ppm [17].

3.3.3. *NH_3 gas PPM variation*

The PPM variation is also considered an active region for the sensor. Fig. 12 represents the sensitivity versus NH_3 gas concentrations at different ppm variations of the $ZrSe_2$ thick film. It is clear from the figure that the gas response goes on increasing linearly with gas concentration.

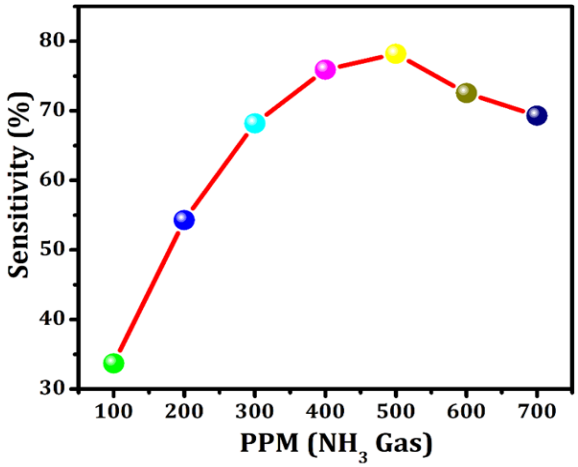

Fig. 12. Graph of sensitivity versus NH_3 gas concentrations (ppm).

It has been found that, as the NH_3 gas concentrations in ppm increased the sensitivity of the film also increased. It might be because the NH_3 gas molecules from that layer would reach the surface active sites of the film hence the sensitivity of the film increased [12].

3.3.4. *Response and recovery time*

The response time is the amount of time it takes for the sensor to change its conductance by 90% of its maximum after being exposed to the test gas. The recovery time is the amount of time it takes the sensor to regain 90% of the initial conductance.

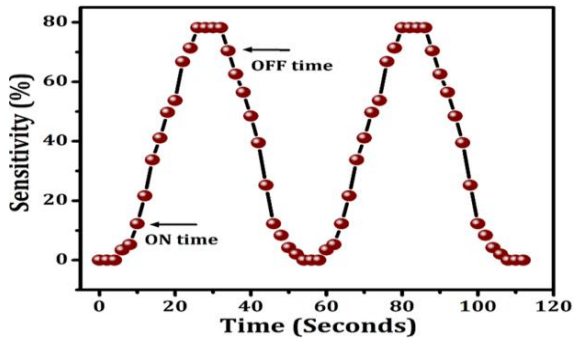

Fig. 13. Response and recovery time.

Fig. 13 shows the response and recovery time of $ZrSe_2$ thick film to NH_3 gas concentration of 500 ppm at the operating temperature of 120°C. The response was rapid (~10 Sec) to 500 ppm of NH_3 gas, whereas the recovery was rapid (~34 Sec). Rapid gas oxidation may be the cause of the speedy response. Its rapid reactivity and rapid return to its desired chemical state are explained by the slight amount of the surface side reaction and its volatility [18].

3.3.5. *Reusability*

The reusability is also one of the important properties of the gas sensor. It indicates the repeatability as well as the durability of the sensor [19]. The reusability of $ZrSe_2$ thick film was studied to NH_3 gas concentration of 500 ppm at the operating temperature of 120°C. The sensitivity of the film was tested or examined over one month and after 5 days. Fig. 14 shows the sensitivity versus number of days.

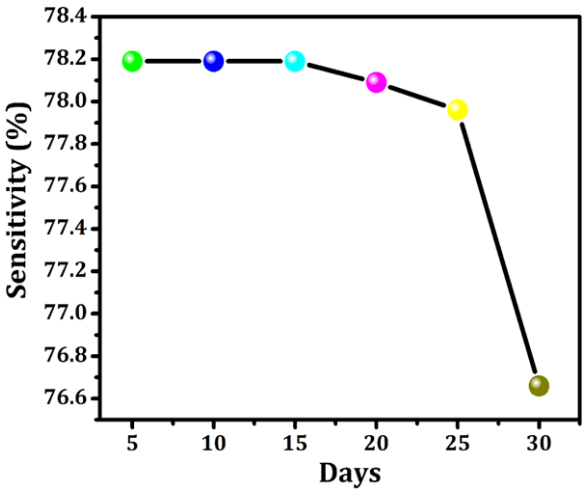

Fig. 14. Reusability of $ZrSe_2$ thick film.

3.4. Gas sensing Mechanism

The variations in electrical resistance are caused by the chemical interactions between the gas molecules and the sensing materials. The processes of adsorption and desorption are all related to the gas interaction with the surface of the nanostructured $ZrSe_2$ thick film sensor [20, 21, 22]. The $ZrSe_2$ is an n-type semiconductor material [5].

Initially, oxygen molecules (O_2 (gas)) in the air are adsorbed physically (O_2 (ads)) on the surface of grains (Eq. 5). As the temperature rises, $ZrSe_2$ chemically adsorbed oxygen molecules, which ionised to form adsorbed oxygen species, such as

[DOI: 10.22068/ijmse.3601]

O^-, O^{2-} and O_2^- (Eq. 6). The selection of the operating temperature affects the formation of various oxygen species. During this process, electrons are trapped from the conduction band of $ZrSe_2$, and a depletion layer is formed on the surface of the $ZrSe_2$ grain, increasing the resistance for $ZrSe_2$ sensors as shown in Fig. 15 (a). The reaction is shown as follows,

$$O_2(gas) \rightarrow O_2(ads) \quad (5)$$

$$O_2(ads) + e^- \rightarrow O_2^-(ads) \ (T < 200℃) \quad (6)$$

As the sensor is exposed to ammonia gas, the adsorbed ammonia molecules react with the initially adsorbed oxygen ions (O_2^-) on the surface, releasing electrons back to the sensing material and reducing the width of the depletion layer (Eq. 7). This increases the electrical conductivity as shown in Fig. 15 (b) [21]. The reaction is shown as follows,

$$4NH_3 + 5O_2^- \rightarrow 4NO + 6H_2O + 5e^- \quad (7)$$

The hierarchical nanostructure of the $ZrSe_2$ materials is responsible for the sensor's excellent sensing abilities. This structure offered many exposed active sites and grain boundaries, which improved the interaction between NH_3 gas and $ZrSe_2$ nanostructure. However, no relevant research on the use of $ZrSe_2$ nanostructured thick films for NH_3 gas detection at various operating temperatures has been found. The current work focuses on the systematic enhancement of $ZrSe_2$ nanostructure thick film for gas sensitivity. The $ZrSe_2$ thick film demonstrates a good sensor response and selectivity for NH_3 gas and shows a fast response and recovery time at 120°C. According to the author's knowledge, this is the first study on the use of $ZrSe_2$ nanostructure for NH_3 gas detection by hydrothermal method.

4. CONCLUSIONS

In this study, successfully synthesized $ZrSe_2$ nanoparticles by hydrothermal method. XRD analysis confirmed that hexagonal Wurtzite-type structure. The SEM analysis revealed the hierarchical nanoparticles surface morphology. The specific surface area is calculated by the BET method and it was found to be 26.86 m^2/gm. The optical band gap of 3.75 eV is revealed by the UV-visible absorption spectra. The $ZrSe_2$ nanoparticles revealed excellent sensitivity, selectivity and good response and recovery properties towards ammonia gas at low operating temperatures. The film shows fast response and recovery time to 500 ppm of NH_3 gas, which is ~10 Sec, and ~34 sec respectively. $ZrSe_2$ nanoparticles appear to be a potential option for ammonia gas sensing applications, based on the results.

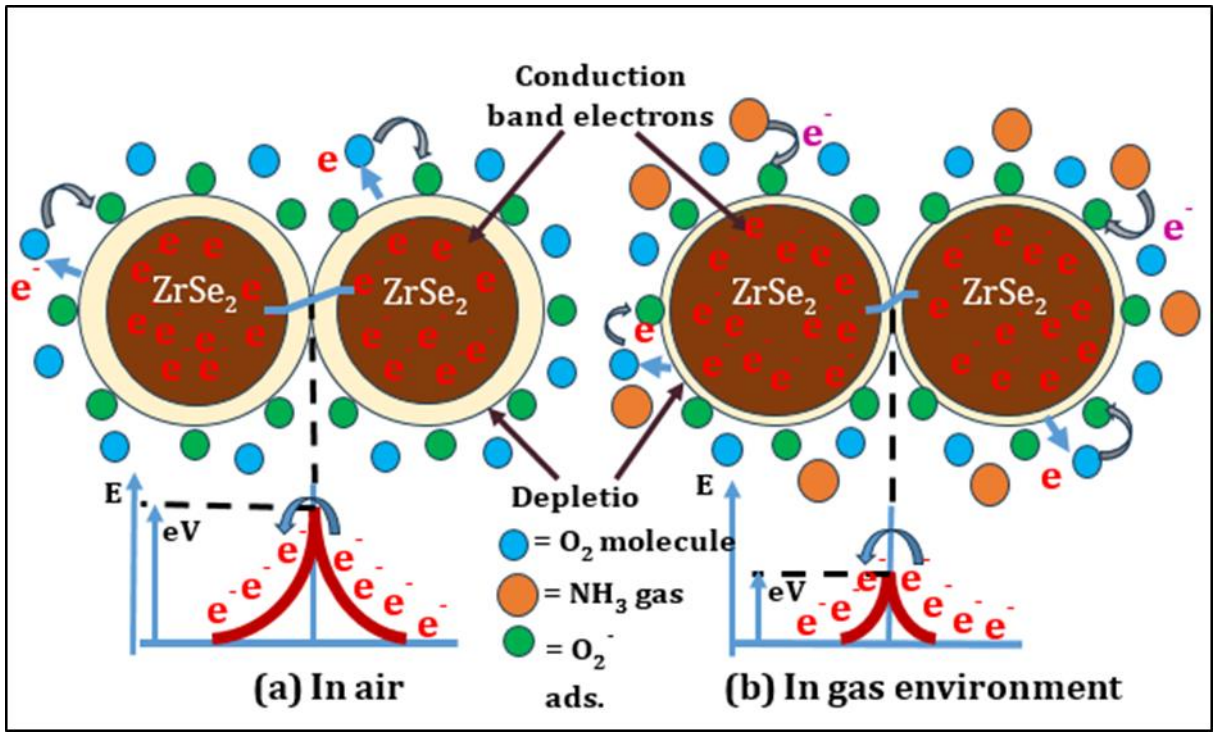

Fig. 15. Schematic representation of the gas sensing mechanism (a) in air and (b) in NH_3 gas Environment

[DOI: 10.22068/ijmse.3601]

ACKNOWLEDGEMENT

We are very much thankful to the Department of Physics and Material Research Laboratory, K.R.T. Arts, B.H. Commerce, A.M. Science College, Nashik, India for providing a lab facility for current research work. I also thank to Principal of DES's Karmaveer Ramraoji Aher ASC College, Deola, for constant guidance and extensive support to encourage this work. We would also thanks to STIC, Cochin University of Science &Technology Campus, Kochi 682 022, Kerala, India and CFC Shivaji University, Kolhapur for characterization facilities.

COMPLIANCE WITH ETHICAL STANDARDS

There is no disclosure of potential conflicts of interest.

DECLARATION OF INTERESTS

The authors declare that they have no known competing financial interests or personal relationships that could have appeared to influence the work reported in this paper.

RESEARCH DATA POLICY AND DATA AVAILABILITY STATEMENTS

Data cannot be shared openly but are available on request from authors.

CREDIT AUTHORSHIP CONTRIBUTION STATEMENT

T. S. Wagh: Conceptualization, Investigation, Data curation, Validation, Writing-original draft.
S. H. Mane: Software, Formal analysis, Methodology.
G. H. Jain: Visualization, Supervision.
M. K. Deore: Supervision, Methodology, Visualization, Review and Editing.

REFERENCES

[1]. Zhang, X., Teng, S. Y., Loy, A. C. M., How, B. S., Leong, W. D. and Tao, X., "Transition metal dichalcogenides for the application of pollution reduction: A review." Nanomaterials, 2020, 10, 1012-1044.

[2]. Shaukat, R. A., Khan, M. U., Saqib, Q. M., Chougale, M. Y., Kim, J., Bermak, A. and Bae, J., "Two-dimensional Zirconium diselenide based humidity sensor for flexible electronics." Sens. Actuators B: Chem., 2022, 358, 131507-131516.

[3]. Ikhioya, L. I., Chime, U. K., Okoro, C. F., Iroegbu, C., Maaza, M. and Ezema, F. I., "Influence of dopant concentration on the electronic band gap energy of Yb-$ZrSe_2$ thin films for photovoltaic application via electrochemical deposition technique." Mater. Res. Express, 2020, 7, 026420-026428.

[4]. Rakkini, A. P. V. and Mohanraj, K., "Effect of different combinations of precursors of zirconium and selenium in the electrodeposited $ZrSe_2$ thin films." Ionics, 2018, 24, 1243-1252.

[5]. Sargar, A. M., Patil, N. S., Mane, S. R., Gawale, S. N. and Bhosale, P. N., "Electrochemical synthesis and characterisation of $ZrSe_2$ thin films." Int. J.Electrochem. Sci., 2009, 4, 887-894.

[6]. Cao, Q., Zhang, J., Zhang, H., Xu, J. and Che, R., "Dual-surfactant templated hydrothermal synthesis of $CoSe_2$ hierarchical microclews for dielectric microwave absorption." J. Adv. Ceram., 2022, 11, 504-514.

[7]. Murugadoss, V., Panneerselvam, P., Yan, C., Guo, Z. and Angaiah, S., "A simple one-step hydrothermal synthesis of cobalt-nickel selenide/graphene nanohybrid as an advanced platinum-free counter electrode for dye-sensitized solar cell." Electrochimica Acta, 2019, 312, 157-167.

[8]. Tupe, U. J., Zambare, M. S., Patil, A. V. and Koli, P. B., "The binary oxide NiO-CuO nanocomposite based thick film sensor for the acute detection of Hydrogen Sulphide gas vapours." Mater. Sci. Res. India, 2020, 17, 260-269.

[9]. Ahire, S. A., Koli, P. B., Patil, A. V., Jagdale, B. S., Bachhav, A. A. and Pawar, T. B., "Designing of screen-printed stannous oxide (SnO_2) thick film sensors modified by cobalt and nitrogen elements for sensing some toxic gases and volatile organic compounds." Curr. Res. Green Sustain. Chem., 2021, 4, 100213-100224.

[10]. Bangale, S. V., Prakshale, R. D. and Bamane, S. R., "Nanostructured $CdFe_2O_4$

[DOI: 10.22068/ijmse.3601]

Thick Film Resistors as Ethanol Gas Sensors." Sensors & Transducers, 2012, 146, 133-144.

[11]. Ikhioya, I. L., Nkele, A. C., Okoro, C. F., Obasi, C., Whyte, G. M., Maaza, M. and Ezema, F. I., "Effect of temperature on the morphological, structural and optical properties of electrodeposited Yb-doped $ZrSe_2$ thin films." Optik, 2020, 220, 165180-165197.

[12]. Choi, W., Choudhary, N., Han, G. H., Park, J., Akinwande, D. and Lee, Y. H., "Recent development of two-dimensional transition metal dichalcogenides and their applications." Mater. Today, 2017, 20, 116-130.

[13]. Hemalatha, E. and Gopalakrishnan, N., "Gas sensing performances of pure and Cu-doped ZrO_2 Nanoparticles." Appl. Phys. A, 2019, 125, 1-12.

[14]. Onkar, S. G., Nagdeote, S. B., Wadatkar, A. S. and Kharat, P. B., "Gas sensing behaviour of ZnO thick film sensor towards H_2S, NH_3, LPG and CO_2." In J. Phys: Conf. Ser., 2020, 1644, 012060-012070.

[15]. Shinde, R. S., Khairnar, S. D., Patil, M. R., Adole, V. A., Koli, P. B., Deshmane, V. V., Halwar, D.K., Shinde, R.A., Pawar, T.B., Jagdale, B.S. and Patil, A. V., "Synthesis and characterization of ZnO/CuO nanocomposites as an effective photocatalyst and gas sensor for environmental remediation." J. Inorg.Organomet. Polym. Mater., 2022, 32, 1-22.

[16]. Balamurugan, C. and Lee, D. W., "A selective NH_3 gas sensor based on mesoporous p-type NiV_2O_6 semiconducting nanorods synthesized using solution method." Sens. Actuators B: Chem., 2014, 192, 414-422.

[17]. Koli, P. B., Kapadnis, K. H., Deshpande, U. G., Tupe, U. J., Shinde, S. G. and Ingale, R. S., "Fabrication of thin film sensors by spin coating using sol-gel $LaCrO_3$ Perovskite material modified with transition metals for sensing environmental pollutants, greenhouse gases and relative humidity." Environmental Challenges, 2021, 3, 100043-100055.

[18]. Gaikwad, S. S., More, M. S., Khune, A. S., Mohammed, H. Y., Tsai, M. L., Hianik, T. and Shirsat, M. D., "Polyvinyl chloride-reduced graphene oxide based chemiresistive sensor for sensitive detection of ammonia." J. Mater. Sci.: Mater.Electron., 2024, 35, 1-18.

[19]. Bagul, V. R., Bhagure, G. R., Ahire, S. A., Patil, A. V., Adole, V. A. and Koli, P. B., "Fabrication, characterization and exploration of cobalt (II) ion doped, modified zinc oxide thick film sensor for gas sensing characteristics of some pernicious gases." J. Indian Chem.Soc., 2021, 98, 100187.

[20]. Zhou, P., Shen, Y., Lu, W., Zhao, S., Li, T., Zhong, X., Cui, B., Wei, D. and Zhang, Y., "Highly selective NO_2 chemiresistive gas sensor based on hierarchical In_2O_3 micro flowers grown on clinoptilolite substrates." J. Alloys Compd., 2020, 828, 154395-154406.

[21]. Zhao, S., Shen, Y., Zhou, P., Hao, F., Xu, X., Gao, S., Wei, D., Ao, Y. and Shen, Y., "Enhanced NO_2 sensing performance of ZnO nanowires functionalized with ultra-fine In_2O_3 nanoparticles." Sens. Actuators B: Chem., 2020, 308, 127729-127737.

[22]. Sharma, N., Sharma, N., Srinivasan, P., Kumar, S., Rayappan, J. B. B. and Kailasam, K., "Heptazine based organic framework as a chemiresistive sensor for ammonia detection at room temperature." J. Mater. Chem. A, 2018, 6, 18389-18395.

[DOI: 10.22068/ijmse.3601]